DEPARTMENT OF COMMERCE
SINCLAIR WEEKS, Secretary

WEATHER BUREAU
F. W. REICHELDERFER, Chief

MONTHLY WEATHER REVIEW

JAMES E. CASKEY, JR., Editor

Volume 85
Number 3

MARCH 1957

Closed May 15, 1957
Issued June 15, 1957

THE USE OF SURFACE PRESSURE AND TEMPERATURE OBSERVATIONS IN UPPER-AIR ANALYSIS

C. W. COCHRANE

U. S. Weather Bureau, Washington, D. C.
[Manuscript received March 29, 1956; revised November 7, 1956]

ABSTRACT

A deepening Low in Texas on November 24, 1952 is selected as a case for studying the more complete use of surface pressures and temperatures in upper-air analysis. To supplement the 2100 CST sea level pressure data, significant pressures taken from station barograms for several hours preceding 2100 CST are corrected for diurnal variation, reduced to sea level, and plotted at appropriate points along lines parallel to the direction of movement of the Low. These additional pressures make it possible to show the steep pressure gradient which caused the rapid pressure rise registered on some of the station barograms. By means of synthetic virtual temperature soundings, additional heights are obtained for the 900- and 800-mb. charts at points where surface data are available and at the same points where barogram data are used on the sea level map. These additional data make it possible to show the steep geopotential gradient at upper levels corresponding to the steep pressure gradient at sea level. Geostrophic winds of 1000 knots or more are indicated by the steep gradient aloft but, by use of the equations of motion, it is found that the air does not remain under the influence of the steep gradient long enough to attain such speeds.

1. INTRODUCTION

One of the trends in recent meteorological thinking has been an increased emphasis on the importance of the mesoscale of analysis. This may be defined as an analysis arrived at by the gleaning of meteorological information between regular reporting stations, as shown in the recent work of Tepper [11, 12] and his associates [3] and in the work of Lott, for example, on intense rainfall situations [6, 7, 8].

There is a wealth of surface pressure data currently available in the form of hourly observations and barograph traces, which can be used to supplement the usual data available for synoptic analysis. Then too, dense networks of surface pressure observation stations or of barographs with speeded-up clocks can be established fairly cheaply. The supplementing of upper-air observations, however, is much more difficult and more expensive. Still, much could evidently be done to refine upper-air analyses by the application of the hydrostatic equation to data available from the denser surface network. It is, of course, by this means that all constant-pressure contours are ultimately derived, since the contour patterns aloft are functions of the surface pressure field and the mean virtual temperature fields of the layers above.

Several recent investigations [1, 2, 4, 5, 9, 10] suggest that the lower levels, perhaps 900 and 800 mb., may be of great importance in some weather phenomena. Improvement in analysis of these surfaces might be achieved by an intensive use of the available surface observations. It is also possible that, through dynamic and synoptic considerations, we may be able to improve our knowledge of the mean temperature fields in the upper air beyond what the data alone give us. This paper, presenting some work done in the course of an investigation of pressure changes, reports on a first attempt to accomplish this aim.

Since errors in the thicknesses of layers bounded by constant-pressure surfaces accumulate with increasing height, the effect of upper-air temperatures on heights of constant-pressure surfaces is relatively less important at low levels than at high levels. A change of 1° C. in the mean virtual temperature of a layer of air 1,800 g.p.m. thick, which is the approximate thickness of the layer from sea level to 800 mb., results in a change in thickness of about 7

g.p.m., provided the sea level pressure remains constant.[1] A change in thickness of about 8 g.p.m. occurs in such a layer at ordinary temperatures when the sea level pressure changes 1 mb., provided the mean virtual temperature of the layer does not change.[2] In this study the use of surface temperatures to help determine upper-level temperatures, on which thicknesses depend, was restricted to regions where the constant-pressure surfaces were near the ground. When a means of getting more accurate mean virtual temperature fields is developed, these fields may be used with the method of dealing with surface pressures described here to provide a more accurate representation of upper-level contours than can now be done by conventional methods.

2. STORM SELECTION

Since the original purpose of the project was the study of pressure changes, the following criteria were set up for selection of a storm situation:

1. A rapidly-deepening Low (pressure falls of 5 mb. per 3 hr. or greater) preferably in the early stages of development.
2. Absence of rainfall.
3. Minimum orographic influence.

A search of surface maps of October through April from the years 1951–52 and 1952–53, as well as some remembered cases as far back as 1947, soon showed that in order to fill requirements 1 and 3, requirement 2 would have to be eliminated. Then, after a second screening on the basis of availability of upper-air reports, the case of a Low in Texas at 2100 CST, November 24, 1952 was finally chosen. The situation is illustrated in figure 1, the routine WBAN analyses at several levels.

This paper reports on only a portion of the originally projected study, namely, the mesometeorological situation which showed up in connection with the Low when close inspection was made of all information available. For example, it was not known beforehand that large pressure rises occurred in the space of a few minutes. Lack of upper-air data at Big Spring and Amarillo was not considered a handicap when the storm was selected. It was later apparent that soundings at these points would have been very helpful in the phase of the study reported on here.

3. STORM ANALYSIS

SEA LEVEL MAP

The path of the principal low center in Texas at sea level for several hours before 2100 CST, November 24, was determined by studying the barograph traces (fig. 2) of all surface observation stations in the area. These were converted to sea level pressure traces by comparison with the hourly observations (sea level) on Weather Bureau

[1] Table 52D, *Smithsonian Meteorological Tables*, 6th Rev. Ed., 1951.
[2] Ibid., Table 57.

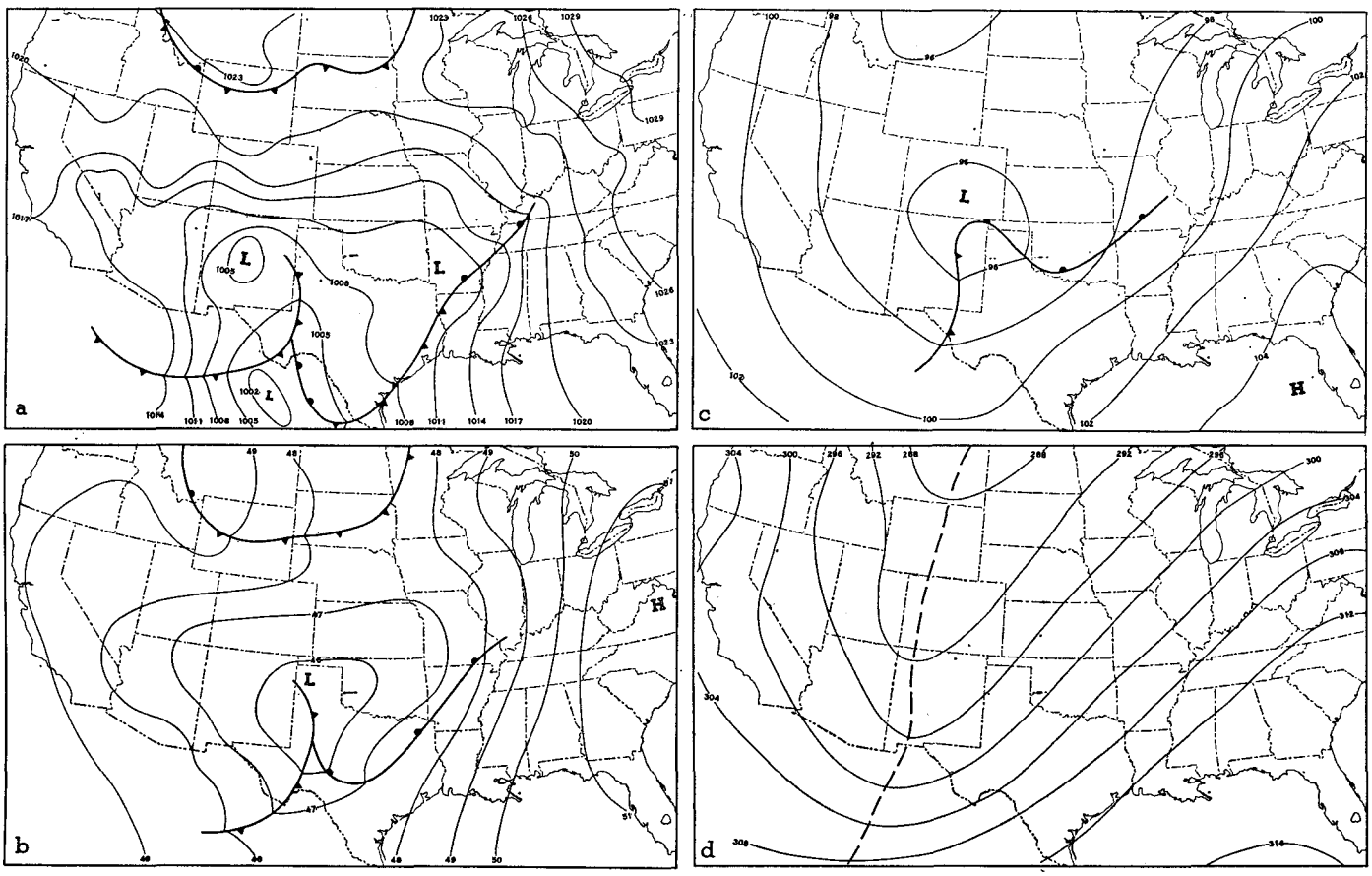

FIGURE 1.—The routinely-made WBAN analyses of the situation of November 24, 1952. (a) Sea level, 1830 CST, (b) 850 mb., (c) 700 mb., and (d) 300 mb., 2100 CST.

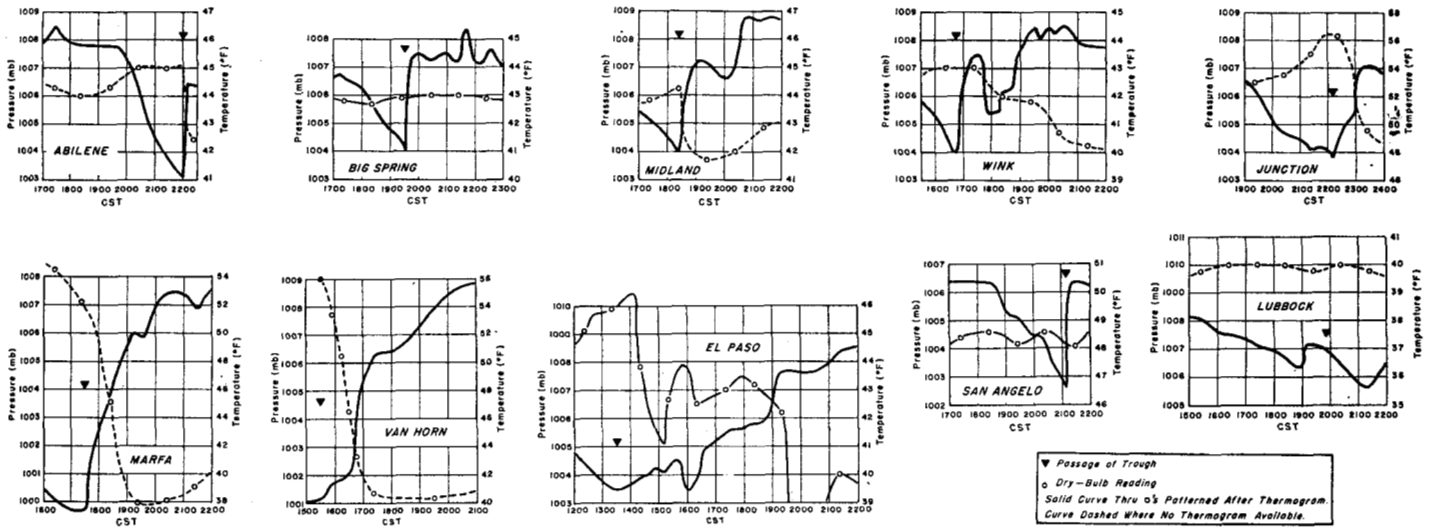

FIGURE 2.—Approximate sea level pressure traces (converted from barograph traces) and surface dry-bulb temperature, at stations in western Texas, November 24, 1952 near the time of passage of the sea level trough at each station.

Forms 1130A. The time of passage of the principal trough was plotted at each station and isochrones drawn at one-hour intervals (fig. 3). The sea level pressure at the time of passage of the principal trough was also plotted at each station and isobars drawn. The axis of minimum pressure of these isobars along a line between Marfa and San Angelo, Tex., is the path taken by the Low center at sea level between 1730 and 2100 CST.

Sea level maps (not all of which are shown) were drawn for each hour from 1830 CST (fig. 4) to 2130 CST, using 1-mb. intervals. A map for 2100 CST (fig. 5) was also drawn by interpolating between the maps for 2030 and 2130 CST. To provide more data in the vicinity of the Low on the hourly maps, maximum and minimum pressures were taken from barograph traces for stations in the area for a couple of hours before and after the passage of the Low. These pressures, reduced to sea level and corrected for the normal diurnal variation between time of occurrence and map time, were plotted along a line through each station parallel to the path of the Low and at distances from the station corresponding to the speed of the Low indicated on the isochronal map. Hourly sea level pressures within a couple of hours of map time, taken from Weather Bureau Forms 1130A, were corrected for diurnal variation and plotted in the same manner.

The additional pressures made possible a more accurate determination of the pressure gradient near the low center than was possible from map-time sea level pressures alone. When they had been analyzed the maps were compared and adjusted so as to effect a regular change in the shape of the low center from one map to the next. Note that a much steeper pressure gradient is shown just west of the trough in western Texas on the sea level map (fig. 4) when information obtained from barograph traces is used and isobars are drawn at 1-mb. intervals, than when only map-time sea level pressures are used and isobars are drawn at 3-mb. intervals, as on the routinely analyzed WBAN Analysis Center map (fig. 1).

CONSTANT PRESSURE AND MEAN VIRTUAL TEMPERATURE CHARTS

Constant-pressure charts for 2100 CST, November 24 were plotted for every 100 mb. from 1000 mb. to 100 mb. Stations with surface pressures lower than 975 mb. were not used on the 1000-mb. chart, and those with station pressures lower than 875 mb. were not used on either the 900- or 1000-mb. charts. Wherever possible, winds for the constant-pressure charts were interpolated between standard levels given in teletypewriter winds-aloft reports.

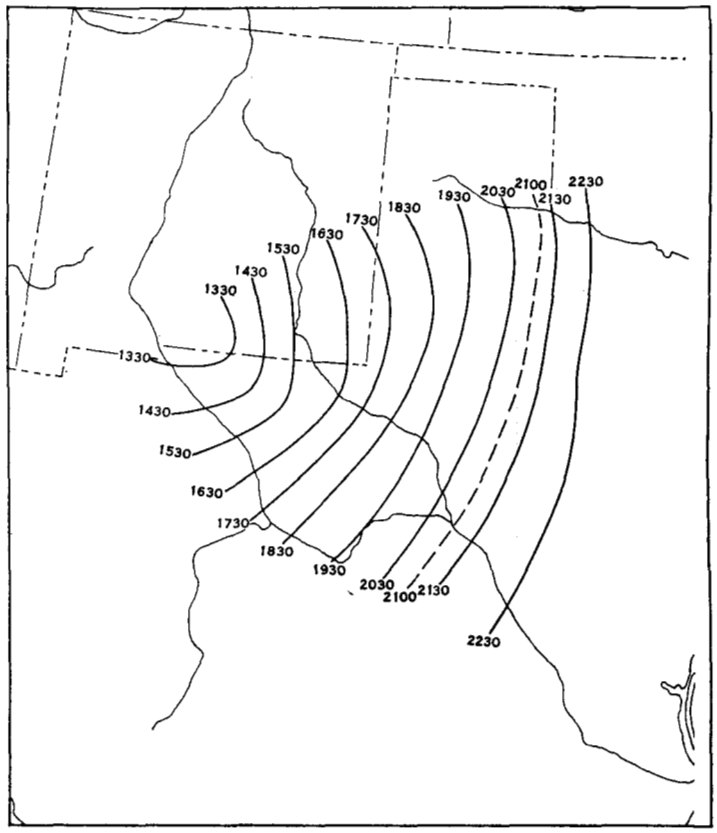

FIGURE 3.—Isochrone chart of passage of trough across western Texas, November 24, 1952. Time is Central Standard Time.

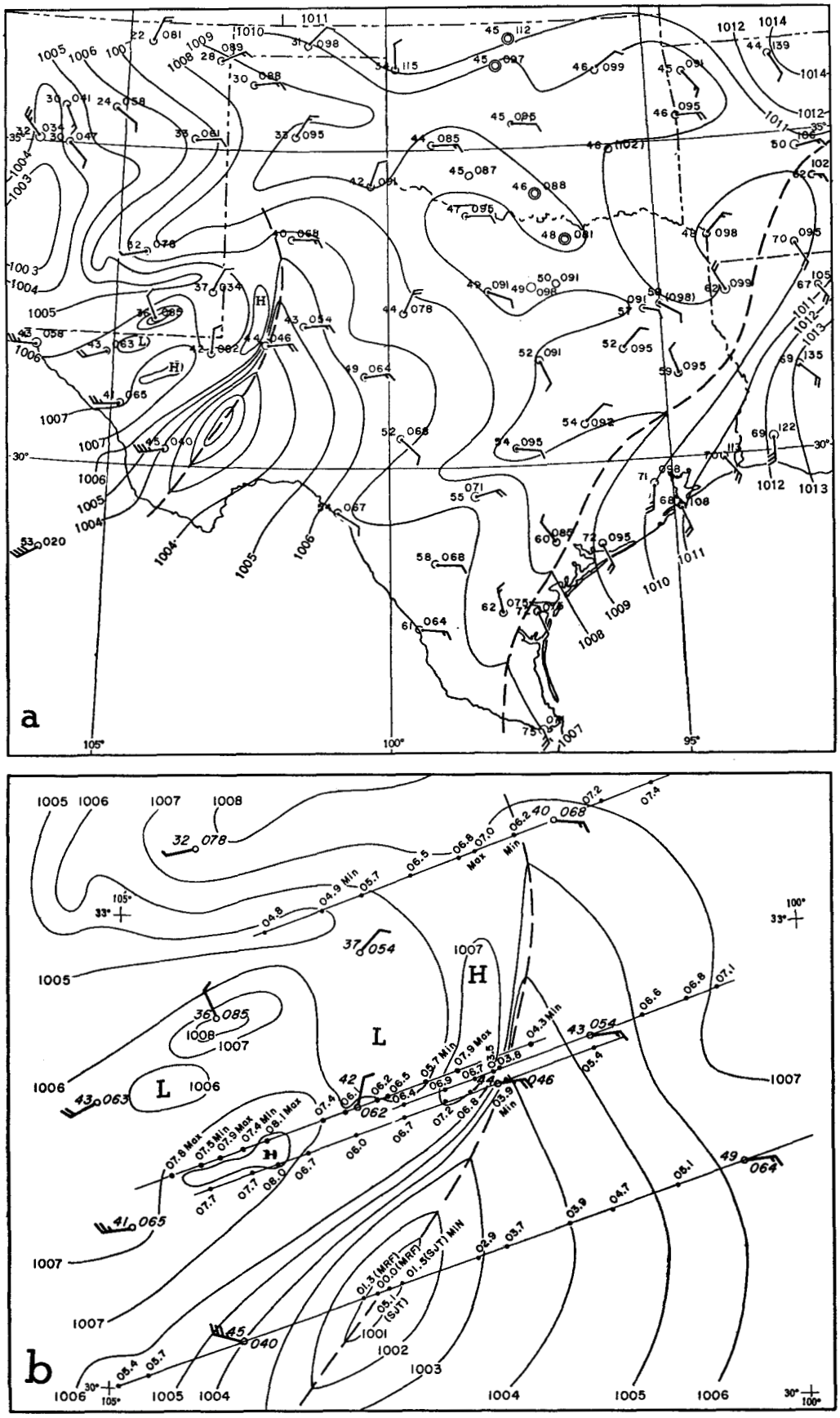

FIGURE 4.—(a) Sea level map for 1830 CST, November 24, 1952, constructed by plotting all surface data available from a variety of sources, and analyzed at 1-mb. intervals. (b) Enlarged section of (a) showing Low and trough line, and maximum, minimum, and hourly pressures (taken from barograph traces for a couple of hours before and after the passage of the Low) plotted parallel to the path of the Low and at distances corresponding to the speed indicated on figure 3.

These winds were plotted, to the nearest 10°, as solid arrows terminating at the station circles, with a short barb equal to 5 knots, a long barb equal to 10 knots, and a pennant equal to 50 knots. For stations for which teletypewriter winds-aloft reports were not available, winds to 16 points were taken from adiabatic charts (WBAN 31A) or from the monthly summary forms (WBAN 33) for each constant-pressure surface and plotted as dashed arrows, using the same scheme for speed as above.

Errors of 1 or 2 g. p. m. were discovered in thicknesses read from the thickness overprint of the adiabatic charts when the overprint was not properly aligned. This results in cumulative height errors of from 10 to 20 g. p. m. at 100 mb. at some stations. However, it should be pointed out that an error of 1° C. in the mean virtual temperature obtained from a representative sounding (Shreveport, La.) would result in errors of 20 g. p. m. in the thickness of the 200–100-mb. layer, 46 g. p. m. in the thickness of the 500–100-mb. layer, and 67 g. p. m. in the thickness of the 1000–100-mb. layer.

Besides the regular upper-air observations, additional heights were obtained for the 1000-, 900-, and 800-mb. charts at stations taking only surface observations. These heights were computed by means of synthetic virtual temperature soundings constructed from surface data and virtual temperature maps (figs. 5–6) drawn at 50-mb. intervals from the upper-air observations at 2100 CST. Figure 7 shows the synthetic sounding for San Angelo, Tex., at 2100 CST, before the sharp pressure rise took place. The soundings for San Antonio and Fort Worth, which are included in figure 7, were used as guides. Figure 7 also shows a possible synthetic sounding for San Angelo at 2112 CST at the end of the sharp pressure rise. This will be discussed below.

In the drawing of the virtual temperature isotherms, a 2° C. interval was used. The surface chart was constructed first since data were most plentiful there. Elevation of the ground was considered in drawing the isotherms in New Mexico and western Texas where data were scarce, assuming a lapse rate of about half the dry-adiabatic. On the 950-mb. chart, a line was drawn showing where the surface pressure was approximately equal to 950 mb. Surface virtual temperatures were then plotted on this line where it intersected the isotherms on the surface chart. At surface observation stations where surface pressures were between 925 and 975 mb. a dry-adiabatic lapse rate was assumed and maximum 950-mb. temperatures obtained for stations with surface pressures less than 950 mb. and minimum values for stations with surface pressures greater than 950 mb.

Marfa, Van Horn, El Paso, and Salt Flat, Tex., were the only stations west of the 2100 CST, November 24 position of the trough where passage of the trough was attended by a marked drop in surface temperature. Except for El Paso, changes in surface temperature were slight and gradual at these and at all other stations in the vicinity of the trough between 1900 and 2200 CST (fig. 2). Hence it appeared that the technique used on the station

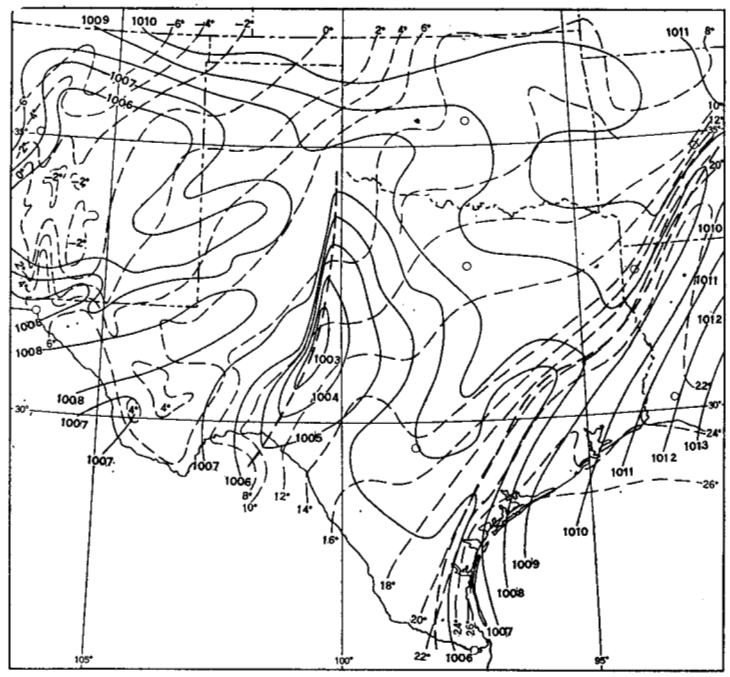

FIGURE 5.—Sea level map for 2100 CST, November 24, 1952, drawn by interpolating between reported data for 2030 and 2130 CST and analyzed at 1-mb. intervals. Dashed lines show surface virtual temperatures in degrees Celsius.

barograms to obtain a better definition of the pressure gradient would be of little help in attempting to define the surface virtual temperature gradient from the station thermograms and humidities. Isotherms were drawn to the virtual temperatures obtained from the upper-air stations and the virtual temperatures at points where the 950-mb. surface intersected the ground, with the maximum and minimum values described above used as guides. A similar procedure was followed on the 900-, 850-, and 800-mb. charts. Synthetic soundings similar to the one for San Angelo at 2100 CST were constructed from these charts at all points on a 1° latitude grid, using actual soundings as guides. Isotherms were then revised where necessary to eliminate, as far as possible, all lapse rates greater than the dry-adiabatic.

Since accurate elevations at each grid point were not known, no heights of constant-pressure surfaces could be computed for these points. However, station barometer heights were known for the surface observation stations and synthetic soundings for these points made it possible to compute 1000-, 900-, and 800-mb. heights at stations with surface pressures equal to or greater than 975 mb., and 900- and 800-mb. heights at stations with surface pressures between 975 and 875 mb.

Still other heights for 900 and 800 mb. were obtained from surface observations in the vicinity of the principal trough in the manner described below. First, two assumptions were made: (1) that the surface pressure at each station in the vicinity of the Low center moved horizontally, at the station barometer elevation, with the direction and speed of the principal trough at the surface, and (2) that the slope of the trough was vertical. (The

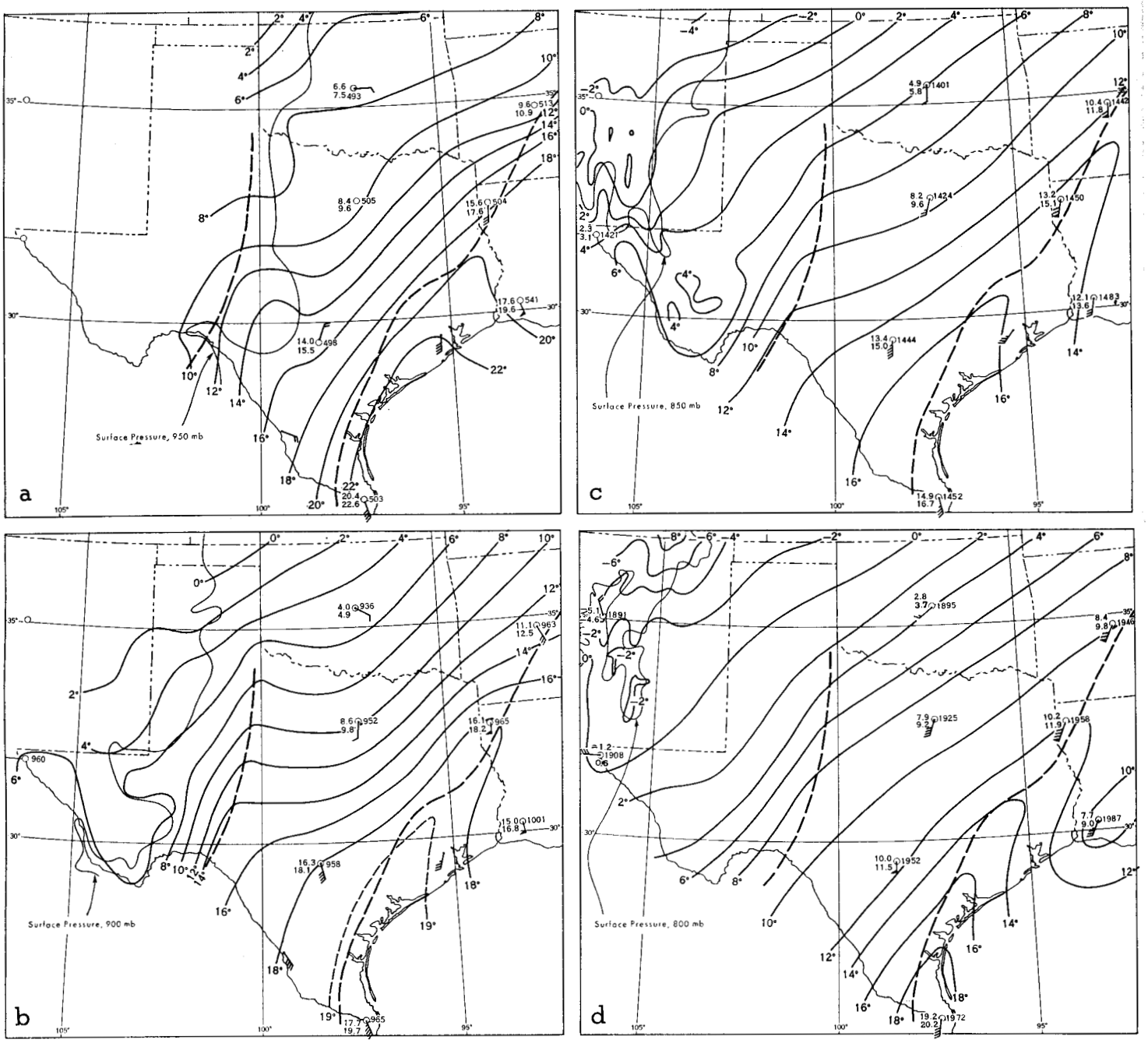

FIGURE 6.—Virtual temperature (° C.) maps for 2100 CST, November 24, 1952 at (a) 950 mb., (b) 900 mb., (c) 850 mb., and (d) 800 mb. In the station model the virtual temperature is plotted below the temperature for the level.

latter assumption was made for the sake of simplicity. Actually, although the surface temperatures at many stations changed very little when the trough passed, colder temperatures to the west aloft indicated that the trough sloped upward at some angle to the west). Then, following a procedure similar to that used on the sea level map, hourly and maximum and minimum surface pressures within a couple of hours of map time were corrected for diurnal variation and plotted along lines through each station parallel to the path of the Low. Synthetic soundings were drawn for these points, using the virtual temperatures from the charts previously mentioned. Thicknesses computed from these soundings were added to station barometer elevations, and the constant-pressure heights so obtained were plotted at the proper points on the 900- and 800-mb. charts. These values were used principally in defining the gradient rather than the actual height at any given point.

CORRELATION OF CONSTANT PRESSURE AND THICKNESS CHARTS

Preliminary contours were drawn on the original constant-pressure charts using a 10-g. p. m. interval from 1000 to 400 mb. and an interval of 20 g. p. m. from 300 to 100 mb. Thickness charts for each 100-mb. layer (1000–900, 900–800, etc.) were plotted (figs. 9–17) and thermal winds constructed.

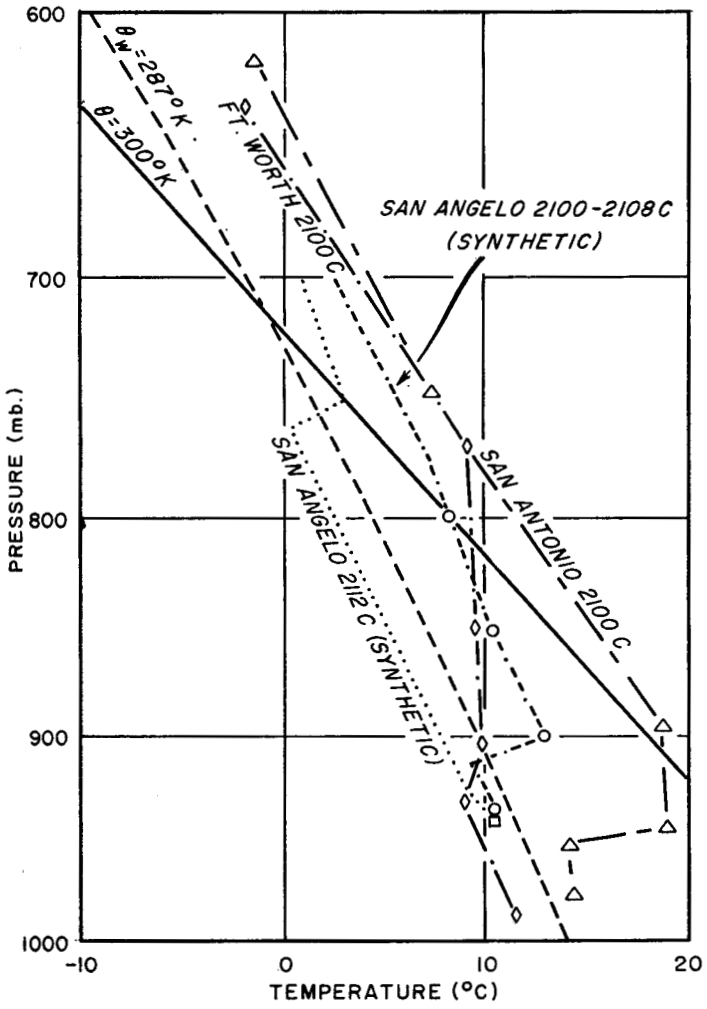

FIGURE 7.—Synthetic upper air sounding for San Angelo, Tex., for 2100 CST, November 24, 1952, before the sharp pressure rise. This sounding was constructed from surface data and the virtual temperature maps (figs. 5, 6). Observed soundings shown for San Antonio and Fort Worth were also used as guides. A second synthetic sounding, for 2112 CST, after the sharp pressure rise, is shown by the dotted line.

Some thermal winds were constructed from teletypewriter winds-aloft reports (direction given to the nearest 10°). Others were constructed from winds reported to 16 points on adiabatic charts (WB Forms 1126). Use of more accurate winds for each constant-pressure surface might have resulted in thermal winds which were in better agreement with thickness lines.

The 1000-mb. constant-pressure chart was subtracted graphically from the 900-mb. chart and thicknesses drawn for every 10 g. p. m. with the plotted thickness values as guides. The thickness lines were smoothed by revising either the 1000- or 900-mb. contours, taking care not to violate any of the plotted data at the upper-air stations. The 900-mb. constant-pressure chart was then subtracted from the 800-mb. chart and smoothing was accomplished by changing the 800-mb. lines where possible. The 900-mb. contours were not revised, however, since that would have necessitated changing the 1000–900-mb. thickness chart. This procedure was repeated up to 100 mb. The final analyses of the constant-pressure charts are shown in figures 8–17.

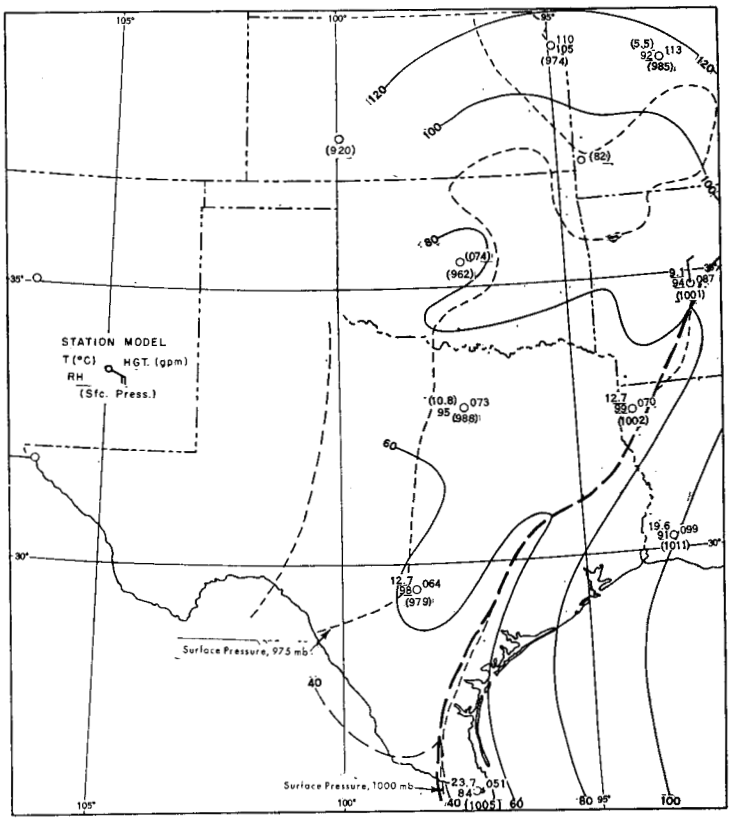

FIGURE 8.—Chart of 1000-mb. height, 2100 CST, November 24, 1952.

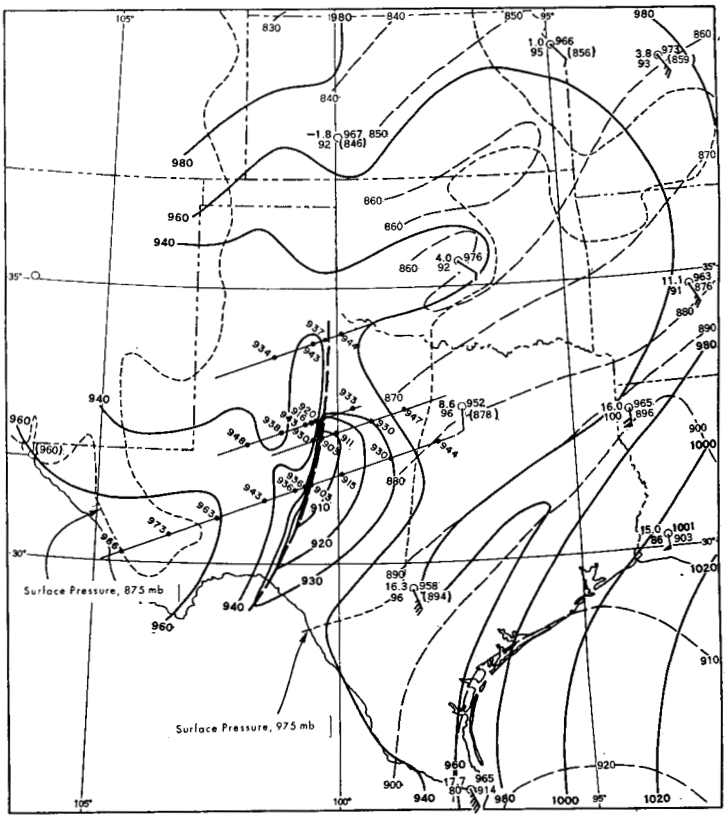

FIGURE 9.—Chart of 900-mb. height (solid lines) and 1000–900-mb. thickness (dashed lines), 2100 CST, November 24, 1952. In the station model thickness is plotted beneath the height; parentheses indicate an extrapolated value. Plotted along the parallel lines are thicknesses computed from synthetic soundings for the maximum, minimum, and hourly pressure points plotted in figure 4b.

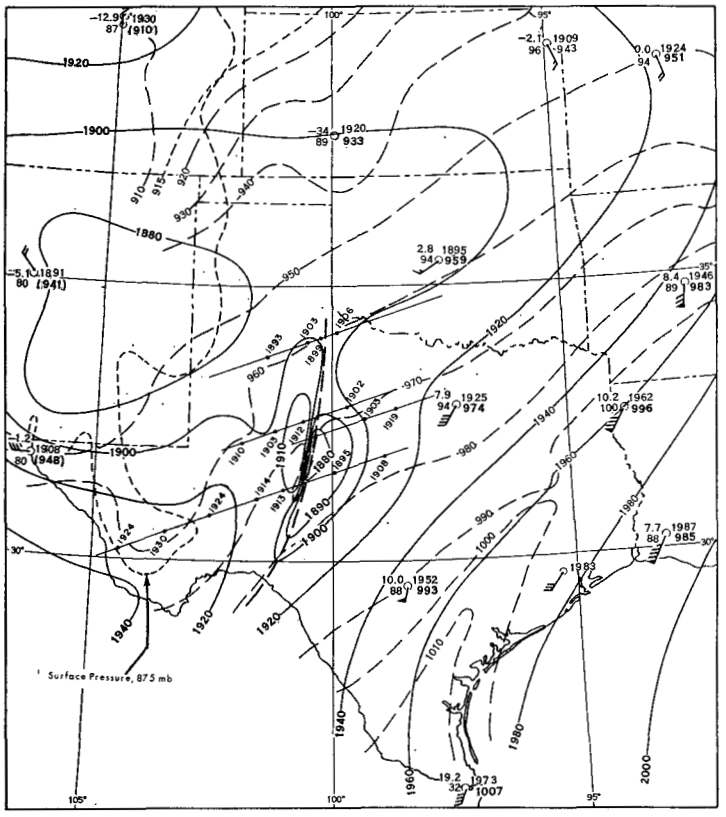

FIGURE 10.—Chart of 800-mb. height (solid lines) and 900–800-mb. thickness (dashed lines), 2100 CST, November 24, 1952.

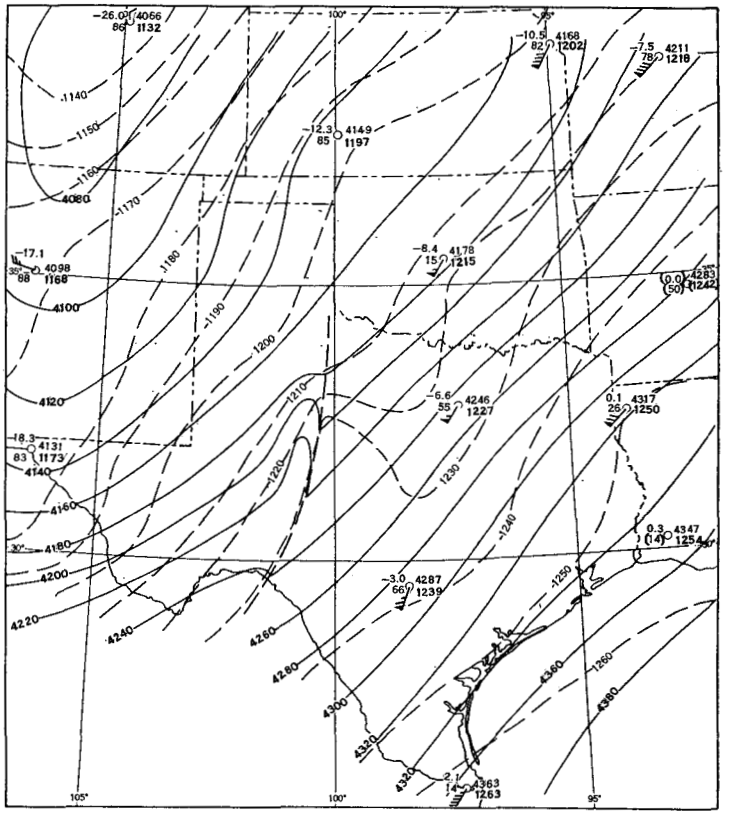

FIGURE 12.—Chart of 600-mb. height (solid lines) and 700–600-mb. thickness (dashed lines), 2100 CST, November 24, 1952.

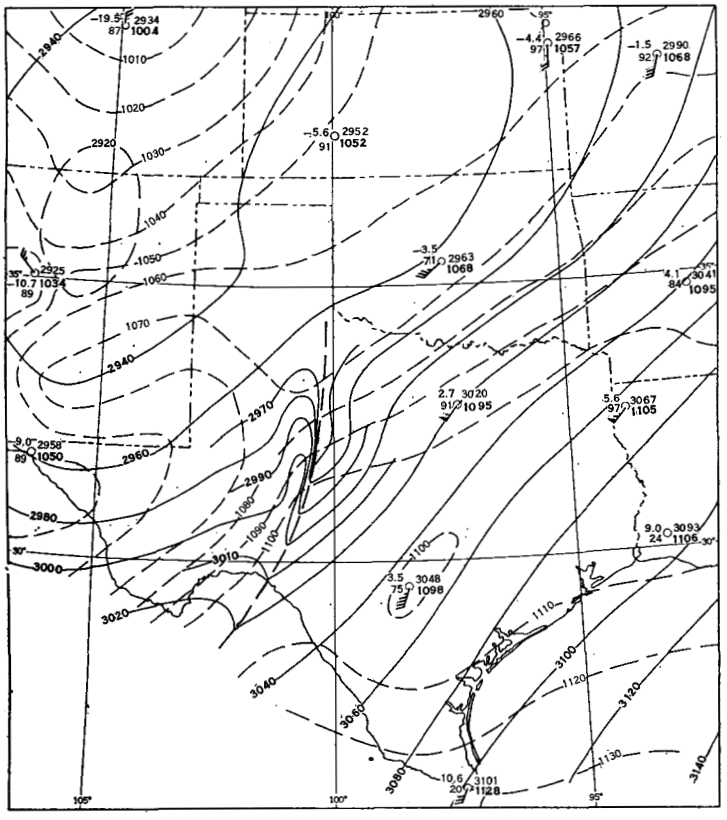

FIGURE 11.—Chart of 700-mb. height (solid lines) and 800–700-mb. thickness (dashed lines), 2100 CST, November 24, 1952.

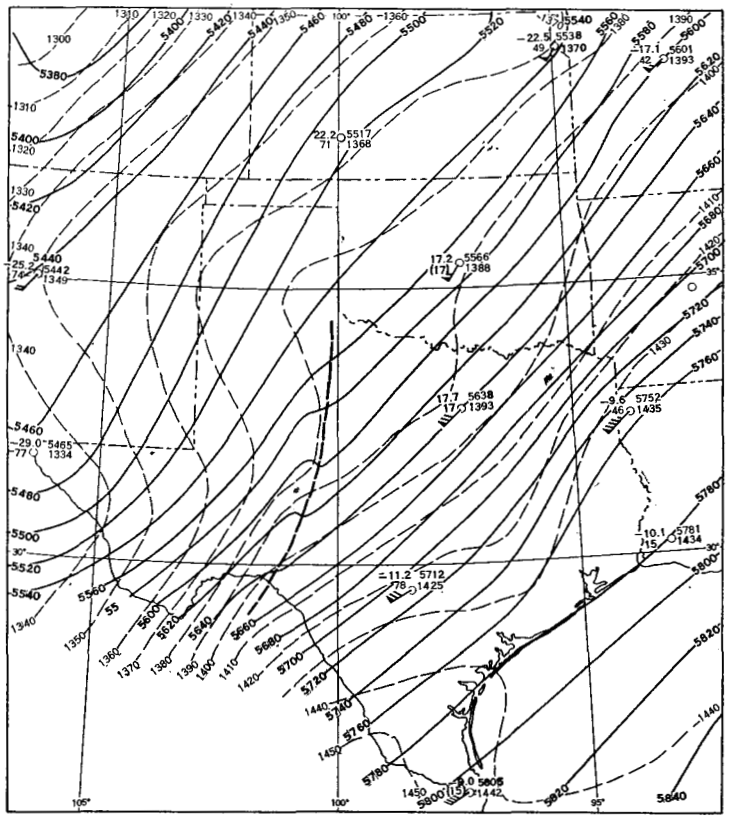

FIGURE 13.—Chart of 500-mb. height (solid lines) and 600–500-mb. thickness (dashed lines), 2100 CST, November 24, 1952.

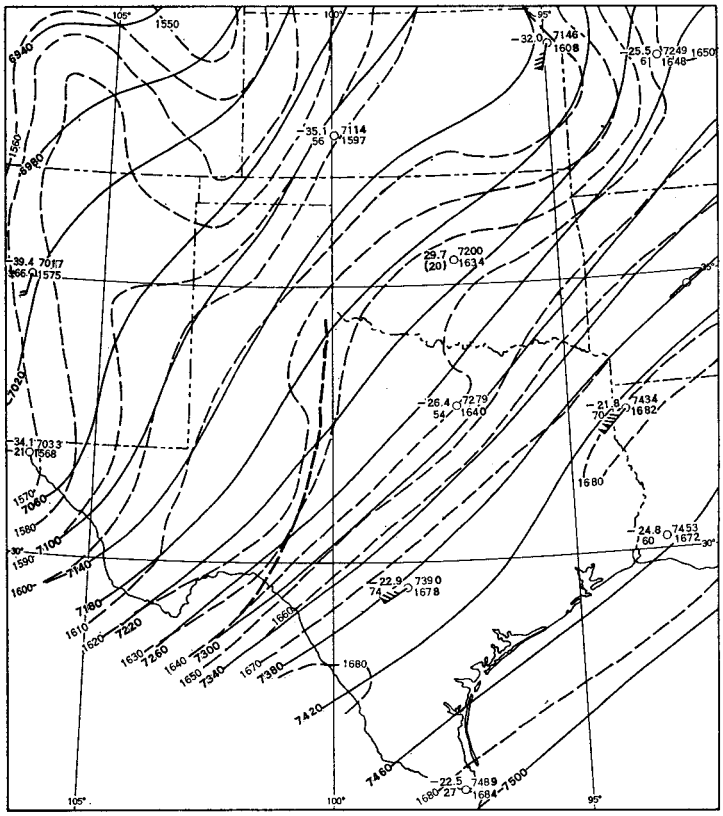

FIGURE 14.—Chart of 400-mb. height (solid lines) and 500–400-mb. thickness (dashed lines), 2100 CST, November 24, 1952.

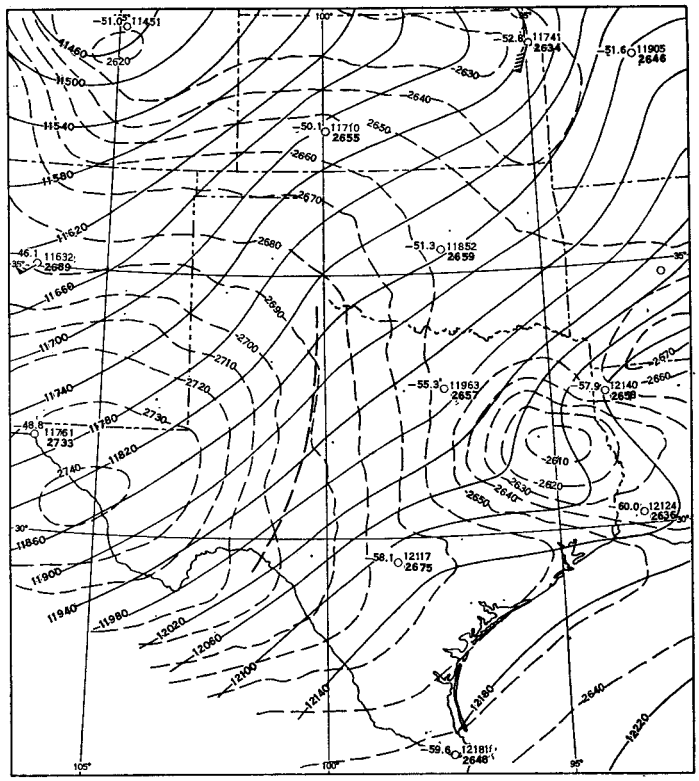

FIGURE 16.—Chart of 200-mb. height (solid lines) and 300–200-mb. thickness (dashed lines), 2100 CST, November 24, 1952.

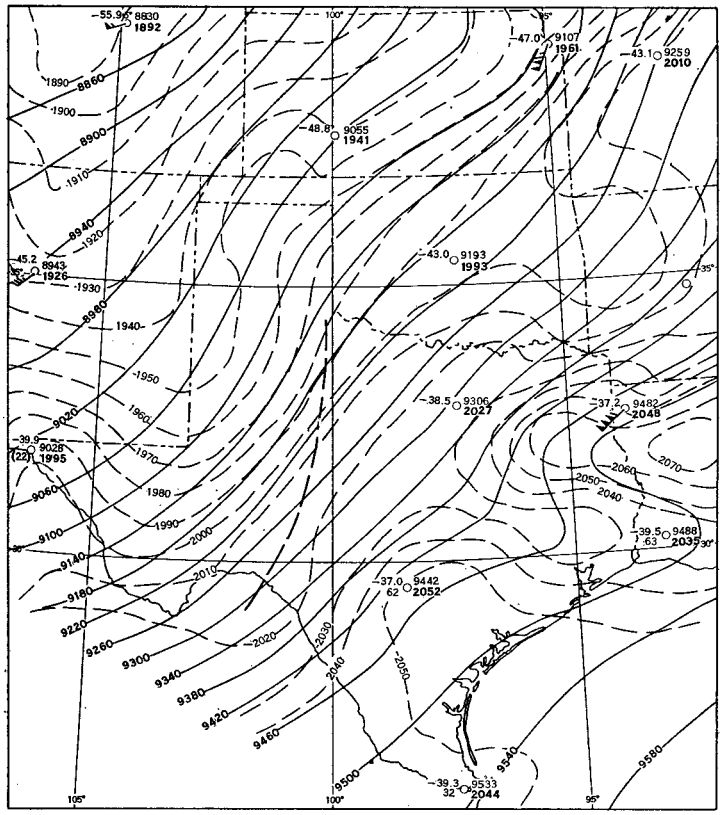

FIGURE 15.—Chart of 300-mb. height (solid lines) and 400–300-mb. thickness (dashed lines), 2100 CST, November 24, 1952.

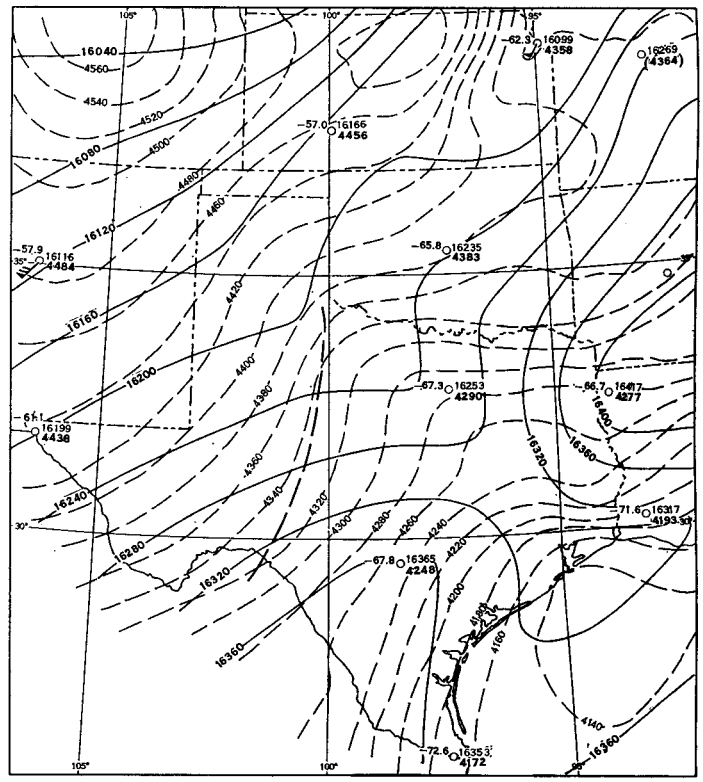

FIGURE 17.—Chart of 100-mb. height (solid lines) and 200–100-mb. thickness (dashed lines), 2100 CST, November 24, 1952.

426194—57——2

The steep pressure gradient in the rear of the trough on the sea level map appears as a steep geopotential gradient on the 900- and 800-mb. charts. This steep gradient extends upward to the 700-mb. chart, becoming weaker at 600 mb., and disappearing at 400 mb.

An interesting feature of the constant-pressure charts, outside the area where barograph data were used, is the change in shape with height of the contours in southeastern Texas and northeastern Kansas. The change begins at about 700 mb. and becomes more pronounced with increasing height, resulting in closed Lows at 100 mb. This is based principally on soundings at Lake Charles and Shreveport, La., Ft. Leavenworth, Kans., and Omaha, Nebr. The contours were spaced mainly to fit the winds at Shreveport and Ft. Leavenworth. Whether the changes in shape of the height lines are real or due to inaccuracies in the winds or heights is not known. Contours on the constant-pressure charts up to 150 mb. drawn by WBAN Analysis Center are smooth in both areas. Figures 1b-d show the 850-, 700-, and 300-mb. charts drawn by WBAN.

EFFECT OF MODIFYING THICKNESS CHARTS

An investigation was made to see how different ways of drawing the thickness charts would affect the height pattern at 600 mb. Lack of upper-air observations in western Texas allowed considerable freedom in drawing thickness lines there. Two sets of 100-mb. thickness charts between 900 and 600 mb. were drawn for the area, assuming very warm temperatures for one set and very

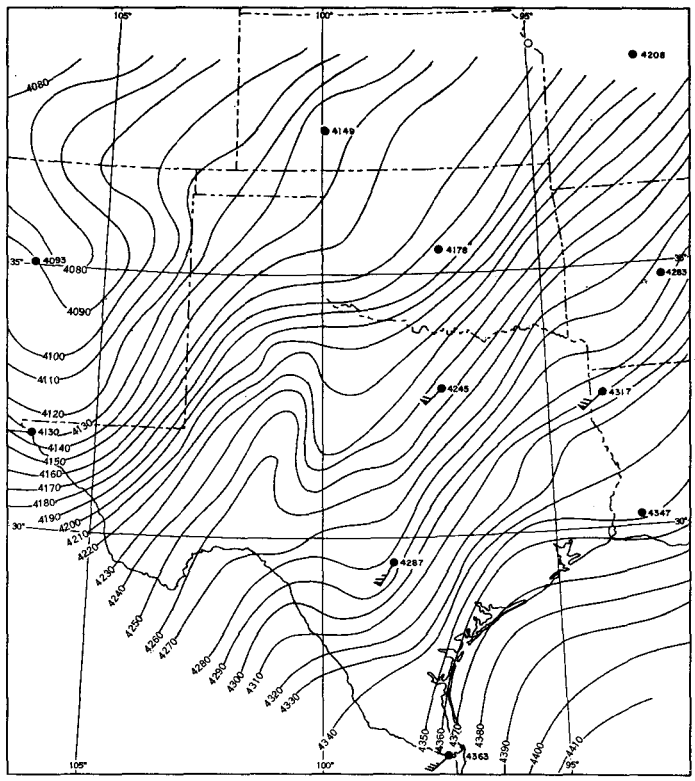

FIGURE 19.—Resulting 600-mb. height chart when thickness between 900 and 600 mb. was computed by 100-mb. intervals from the very warm virtual temperatures.

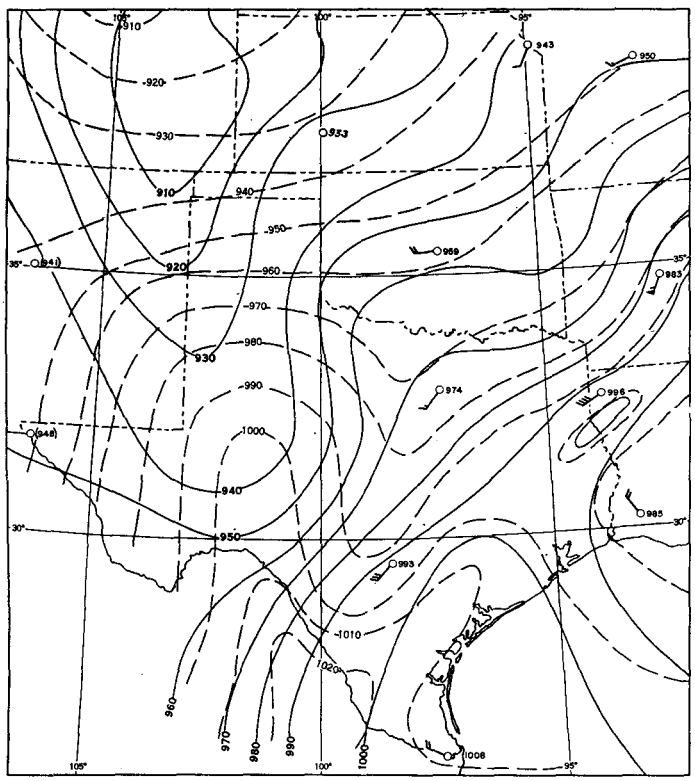

FIGURE 18.—Chart of thickness of 900–800-mb. layer computed from assumed very warm virtual temperatures (dashed lines) and from assumed very cold virtual temperatures (solid lines).

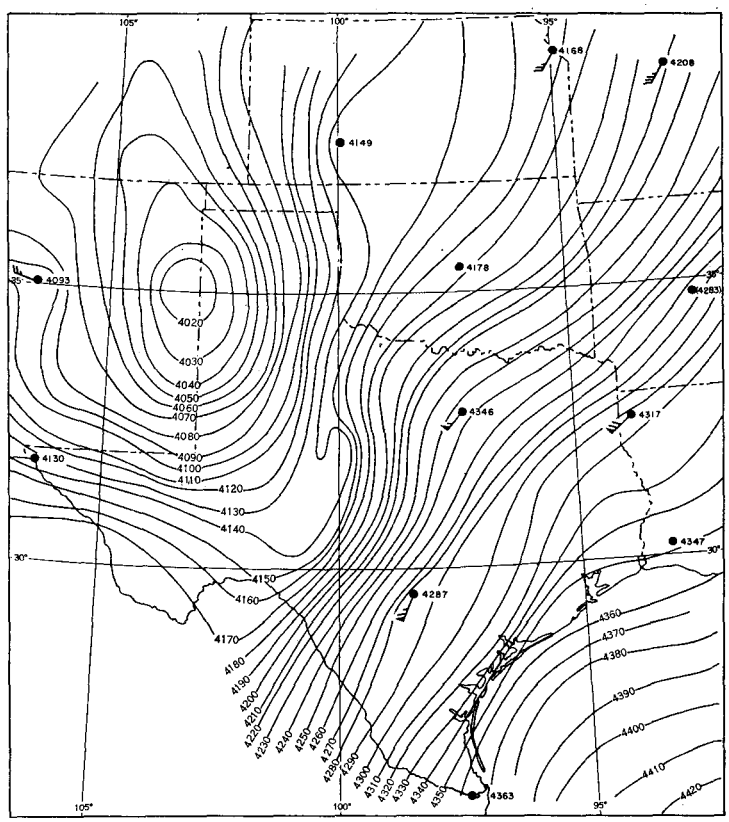

FIGURE 20.—Resulting 600-mb. height chart when 900–600-mb. thickness was based on very cold virtual temperatures.

cold temperatures for the other. Only the 900–800-mb. chart is shown here (fig. 18). These thicknesses were added to the original 900-mb. height chart to obtain two height charts at 600 mb., one from the use of the warm thickness charts (fig. 19) and one from the cold (fig. 20).

Comparison of the two 600-mb. charts shows the point of greatest height difference (136 g. p. m.) to be in the vicinity of Big Spring, Tex. However, some of the thicknesses are too great or too small as drawn, because they indicate lapse rates greater than the dry-adiabatic. Figure 21 shows synthetic soundings for Big Spring, Tex. between 900 and 600 mb., as drawn from mean virtual temperatures corresponding to thicknesses taken from the charts for the very warm and very cold cases. These curves could be drawn in other ways, using the same mean virtual temperatures, but lapse rates would have to be superadiabatic at some points.

In the cold case, a dry-adiabatic lapse rate through the 900-mb. temperature makes the mean virtual temperature 3.0° C. for the 900–800-mb. layer. This would make the thickness 952 g. p. m. instead of 936 g. p. m. as shown. In the warm case, a dry-adiabatic lapse rate through the 800-mb. temperature results in a mean virtual temperature of 14.3° C. for the 900–800-mb. layer. This would make the thickness 992 g. p. m. instead of 997 g. p. m. as shown.

The synthetic sounding actually used for Big Spring is also shown in figure 21. This has been drawn from virtual temperatures taken from the virtual temperature charts for the surface, 900, 850, and 800 mb. and mean virtual temperatures corresponding to thicknesses of the 800–700-mb. and 700–600-mb. layers.

Another investigation was made of the effect on the 800-mb. height pattern if several different 900–800-mb. thickness patterns were added to the original 900-mb. height pattern. Since some of the mean virtual temperatures in the cold case of the first investigation were too low, a 900–800-mb. thickness chart was drawn, assuming a dry-adiabatic lapse rate from the surface to 800 mb. at stations in southeastern New Mexico and Texas west of the trough. Addition of these thicknesses to the original 900-mb. heights resulted in an 800-mb. height chart which was very similar to the original (fig. 10) except that the meso-High associated with the meso-Low near San Angelo, Tex. was slightly weaker.

Another 900–800-mb. thickness pattern was constructed from a mean virtual temperature chart showing a very steep gradient immediately to the west of the trough near San Angelo. This pattern was tried because the surface pressure at San Angelo rose from 935.5 to 939.4 mb. between approximately 2108 and 2112 CST, November 24, and this rapid rise of nearly 4 mb. could be accounted for by a drop of about 5° C. in the virtual temperature between 900 and 760 mb., with smaller drops between 760 and 700 mb. and between 900 mb. and the ground, assuming no change in the 700-mb. height (fig. 7). A decrease of about 2° C. in the mean virtual temperature of a layer about 4,700 g. p. m. thick (900–500 mb.) would also cause a rise of about 4 mb. at levels near 900 mb., assuming no change in the 500-mb. height.

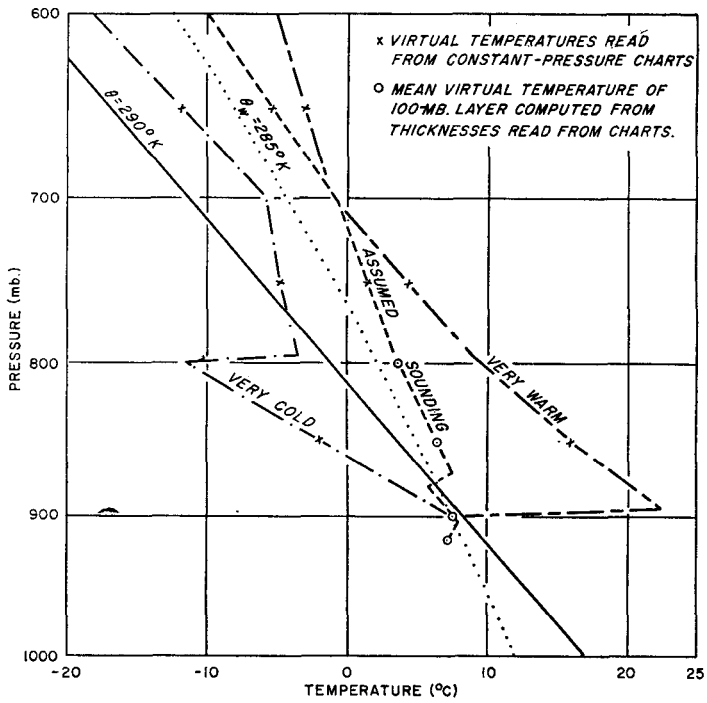

FIGURE 21.—Synthetic soundings for Big Spring, Tex., as drawn corresponding to thicknesses taken from charts for the assumed very warm and very cold virtual temperatures.

It should be pointed out that at San Antonio the mean virtual temperature of the 950–850-mb. layer dropped about 6° C. between the soundings for 2100 CST November 24 and 0900 CST, November 25. The trough passed San Antonio at about 0130 CST, November 25 and the surface pressure rose about 1.4 mb. between 0130 and 0142 CST.

As in the case where dry-adiabatic lapse rates were assumed, in this case also where a very steep temperature gradient was assumed just west of the trough in the 900–800-mb. layer, the 800-mb. height chart resulting from adding this thickness pattern to the original 900-mb. heights turned out to be very similar to the original 800-mb. height pattern, except that the meso-Low was slightly deeper and the meso-High to the west was a little weaker.

Although some of the assumed temperatures were too warm in the case for which very warm mean virtual temperatures were assumed, this case also resulted in a meso-Low on the trough north of San Angelo, Tex. at 800 mb. This Low, however, was much weaker than that shown on the original 800-mb. chart.

To smooth out the pattern by eliminating the meso-Low entirely at 800 mb., the 800-mb. height at San Angelo would have to be raised from 1884 to 1920 g. p. m. Since the 900-mb. height at San Angelo is 906 g. p. m. on the original chart, the 900–800-mb. thickness would have to change from 978 g. p. m., corresponding to an assumed mean virtual temperature of 10.3° C., to 1014 g. p. m. corresponding to a mean virtual temperature of

21.0° C. The latter temperature is much higher than anything indicated by the nearest soundings. For example, San Antonio had a mean virtual temperature of 14.7° C. and Brownsville 18.8° C. for this layer.

Hence, all of the above reasonable assumptions of the distribution of mean virtual temperature of the 900–800-mb. layer indicate that the meso-Low near San Angelo and its associated meso-High to the west still existed at 800 mb.

For the height pattern to be smoothed out at 700 mb. it would be necessary to raise the height at San Angelo from 2980 g. p. m., as shown on the original chart, to about 3003 g. p. m. The original 800-mb. height is 1884 g. p. m. and the original 800–700-mb. thickness 1096 g. p. m., corresponding to a mean virtual temperature of 7.2° C. Increasing the thickness 23 g. p. m. to 1119 g. p. m. would require a rise in mean virtual temperature of the 800–700-mb. layer to 13.1 °C. From the available upper-air winds and temperatures it does not appear likely that such warm air would have reached the vicinity of San Angelo in the 800–700-mb. layer at 2100 CST, November 24. For example, although Brownsville had a mean virtual temperature of 15.3° C. for this layer, San Antonio, which is much closer to San Angelo, had a mean virtual temperature of only 7.7° C.

4. TRAJECTORIES IN REGION OF STEEP GEOPOTENTIAL GRADIENT

The steep geopotential gradient shown on the 900-, 800-, and 700-mb. charts (figs. 9–11) in a narrow band just to the west of the principal trough in western Texas indicated geostrophic winds of 500 to 1000 knots or more. This steep gradient does not appear on the routinely analyzed 850- and 700-mb. charts prepared by the WBAN Analysis Center (fig. 1b, c). Some short-period trajectories near the Low center were constructed to provide estimates of how long the air remained under the influence of the steep gradient. The method of constructing the trajectories is described in the Appendix.

Figure 22 shows as solid lines nine 60-minute trajectories (points A-I) so constructed for the 800-mb. surface, using 10-, 20-, and 30-minute intervals. For comparison, trajectories for points A, E, G, and H, constructed assuming instantaneous response of the parcel to the changing geopotential gradient, are shown as dotted lines. The three dashed lines in figure 22 show the trough position at 30-minute intervals from 2100 to 2200 CST.

It can be seen that air parcels such as those starting from E and G and passing into the region of steep geopotential gradient tended to move with no marked change in velocity and, within 20 minutes or so, passed through the steep gradient and entered regions where the gradient was more nearly normal. (Also see Appendix.)

Assuming approximately horizontal movement, the parcel at point D started ahead of the trough but was overtaken by the trough after about 20 minutes. It gradually accelerated and, 30 minutes later, went ahead of the trough again.

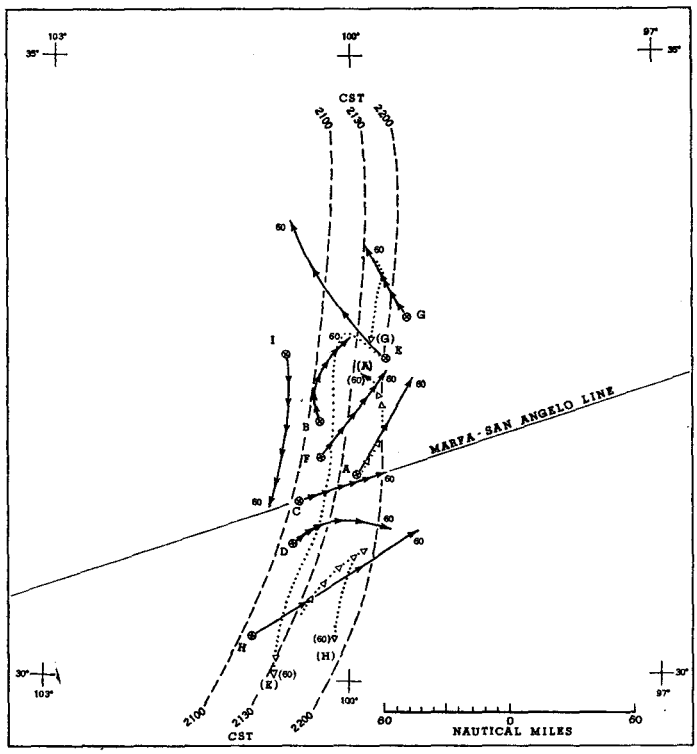

FIGURE 22.—60-minute trajectories (solid arrows) at 800 mb. for parcels under the influence of the steep gradient. For comparison trajectories constructed assuming instantaneous response to the geopotential gradient are shown as dotted lines with open arrow heads for points A, E, G, and H. Position of trough at 30-minute intervals is shown by dashed curves.

An example given in the Appendix makes it easier to see qualitatively the effect on an air parcel moving relatively slowly when it enters the region of steep geopotential gradient.

These short-period trajectories show that it is very unlikely that any one air parcel ever remained under the influence of the steep gradient long enough to attain speeds comparable to the indicated geostrophic winds.

5. CONCLUSIONS

1. Data currently available can be used to provide a much more detailed analysis, both at the surface and aloft, than can be made by techniques developed up to the present time.

2. There is need to develop new techniques, to simplify and systematize them, and to make them speedy enough to be used in routine analysis.

3. The speed of response of the wind to a changing pressure gradient is not rapid. The time of response is of the order of hours rather than of minutes and seconds.

ACKNOWLEDGMENTS

This work was initiated and directly supervised by Dr. Charles S. Gilman, Chief of the Hydrometeorological Section. Selection of the storm was made by Mr. George A. Lott. Mr. William W. Swayne constructed the charts showing the difference at 600 mb. resulting

from the use of very warm and very cold mean virtual temperatures between 900 and 600 mb. Mr. Lott and Mr. Vance A. Myers made several valuable suggestions in the preparation of the paper.

REFERENCES

1. James F. Appleby, "Trajectory Method of Making Short-Range Forecasts of Differential Temperature Advection, Instability, and Moisture," *Monthly Weather Review*, vol. 82, No. 11, Nov. 1954, pp. 320–334.
2. Robert G. Beebe, "Forecasting Winter Precipitation for Atlanta, Ga.," *Monthly Weather Review*, vol. 78, No. 4, Apr. 1950, pp. 59–68.
3. T. Fujita, H. Newstein, and M. Tepper, "Mesoanalysis, An Important Scale in the Analysis of Weather Data," *Research Paper* No. 39, U. S. Weather Bureau, Washington, 1956, 83 pp.
4. George C. Holzworth and Charles F. Thomas, "Low Level Warm Air Advection, June 8–9, 1953," *Monthly Weather Review*, vol. 81, No. 6, June 1953, pp. 169–178.
5. G. A. Lott, "An Extraordinary Rainfall Centered at Hallett, Okla.," *Monthly Weather Review*, vol. 81, No. 1, Jan. 1953, pp. 1–10.
6. G. A. Lott, "The Great-Volume Rainstorm at Elba, Alabama," *Monthly Weather Review*, vol. 82, No. 6, June 1954, pp. 153–159.
7. G. A. Lott, "The Unparalleled Thrall, Texas Rainstorm," *Monthly Weather Review*, vol. 81, No. 7, July 1953, pp. 195–203.
8. G. A. Lott, "The World-Record 42-Minute Holt, Missouri, Rainstorm," *Monthly Weather Review*, vol. 82, No. 2, Feb. 1954, pp. 50–59.
9. Lynn L. Means, "On Thunderstorm Forecasting in the Central United States," *Monthly Weather Review*, vol. 80, No. 10, Oct. 1952, pp. 165–189.
10. Lynn L. Means, "A Study of the Mean Southerly Wind-Maximum in Low Levels Associated with a Period of Summer Precipitation in the Middle West," *Bulletin of the American Meteorological Society*, vol. 35, No. 4, Apr. 1954, pp. 166–170.
11. M. Tepper, "The Application of the Hydraulic Analogy to Certain Atmospheric Flow Problems," *Research Paper* No. 35, U. S. Weather Bureau, Washington, Oct. 1952, 50 pp.
12. M. Tepper, "A Proposed Mechanism of Squall Lines: The Pressure Jump Line," *Journal of Meteorology*, vol. 7, No. 1, Feb. 1950, pp. 21–29.

APPENDIX

The equations used for constructing the trajectories were derived from the following equations of motion for frictionless flow in a constant-pressure surface, with neglect of vertical motions and terms involving the curvature of the Earth's surface:

$$\frac{du}{dt}=f(v-v_g) \tag{1}$$

$$\frac{dv}{dt}=-f(u-u_g) \tag{2}$$

where u=west component of velocity
v=south component of velocity
t=time
$f=2\Omega \sin\varphi$=Coriolis parameter
Ω=angular velocity of Earth
φ=latitude
$u_g=-\frac{1}{f}\frac{\partial\Phi}{\partial y}$=west component of geostrophic velocity
$v_g=\frac{1}{f}\frac{\partial\Phi}{\partial x}$=south component of geostrophic velocity
Φ=geopotential
x,y=Cartesian coordinates, positive toward the east and north, respectively.

For a short time interval, τ, the derivatives on the left side of equations (1) and (2) may be approximated by finite differences in u and v, respectively, over the interval τ, and the instantaneous velocity components on the right sides by the mean of the initial and final values for a parcel during the interval τ. With the neglect of variations in f during the interval, these substitutions in equations (1) and (2) give:

$$\frac{u_n-u_{n-1}}{\tau}=f\left(\frac{v_n+v_{n-1}}{2}-\frac{v_{gn}+v_{g(n-1)}}{2}\right) \tag{3}$$

$$\frac{v_n-v_{n-1}}{\tau}=-f\left(\frac{u_n+u_{n-1}}{2}-\frac{u_{gn}+u_{g(n-1)}}{2}\right) \tag{4}$$

where the subscripts $n-1$ and n denote values at times $t=(n-1)\tau$ and $t=n\tau$, respectively.

The simultaneous solution of (3) and (4) gives

$$u_n=a\,u_{n-1}+2b\,v_{n-1}+c(u_{gn}+u_{g(n-1)})-b\,(v_{gn}+v_{g(n-1)}) \tag{5}$$

$$v_n=a\,v_{n-1}-2b\,u_{n-1}+c(v_{gn}+v_{g(n-1)})+b(u_{gn}+u_{g(n-1)}) \tag{6}$$

where

$$a=\frac{4-f^2\tau^2}{4+f^2\tau^2},\ b=\frac{2f\tau}{4+f^2\tau^2},\ c=\frac{f^2\tau^2}{4+f^2\tau^2}.$$

The use of equations (5) and (6) to compute u_n and v_n for each time step of the trajectory requires that the actual and geostrophic wind components on the right sides be known. The geostrophic wind components were measured on appropriate maps, and the actual wind components were available for each time step, except the first, from the computations of the preceding step. Since an observed wind was not available at most points selected as trajectory origins, the actual wind components on the right side of each equation were replaced, for the initial time only, by the corresponding geostrophic wind components.

In the construction of the trajectories shown in figure 22, it was first necessary to select some initial points on the ground such that air parcels starting above at least a few of these points and moving approximately horizontally over the 800-mb. surface would travel into the region of steep geopotential gradient in a reasonable time. Point B is such a point. In constructing the trajectory originating there, u_{g0} and v_{g0} were measured at the point after aligning the 2100 CST ($t=0$) position of the trough on the trajectory sheet with the 2100 CST position of the trough on the 800-mb. chart. The trajectory sheet was then moved backward along the Marfa-San Angelo line until

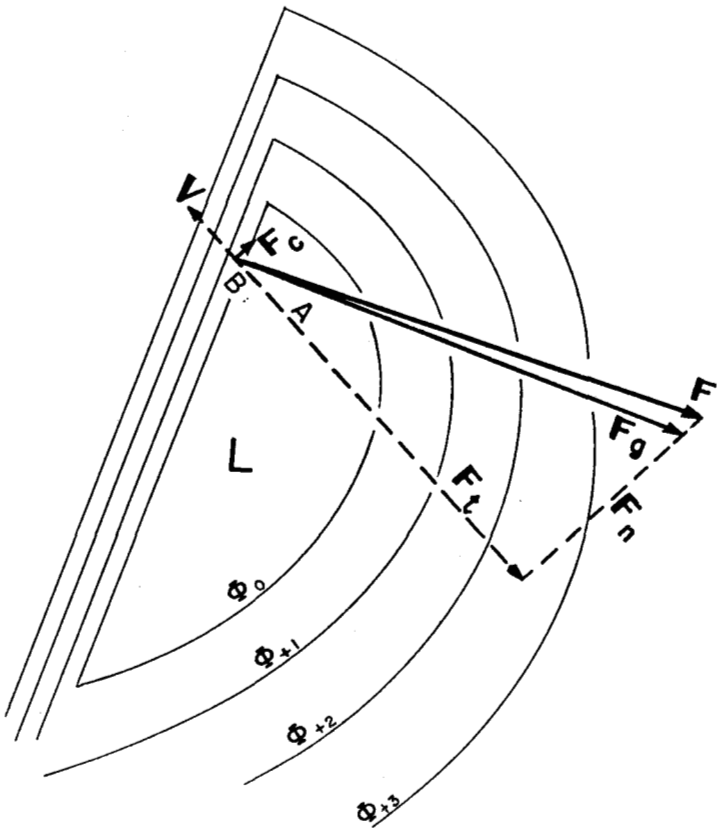

FIGURE 23.—Horizontal forces at work on a parcel of air entering at B a region of steep geopotential gradient.

the 2105 CST $\left(t=\frac{\tau}{2}=5 \text{ min.}\right)$ position of the trough was approximately aligned with the 2100 CST trough position on the 800-mb. chart. Here, $u_{g1/2}$ and $v_{g1/2}$ were measured at point B and used to construct the first approximate trajectory from point B for the first 10 minutes. The trajectory sheet was then moved backward along the Marfa-San Angelo line until the 2110 CST ($t=\tau=10$ min.) position of the trough was approximately aligned with the 2100 CST position on the 800-mb. chart. Here, u_{g1} and v_{g1} were measured at the end of the assumed trajectory. Using u_{g0}, v_{g0}, u_{g1}, v_{g1}, and the mean latitude of the trajectory to the nearest degree, u_1 and v_1 were computed from equations (5) and (6) (with u_0 and v_0 replaced by u_{g0} and v_{g0} as explained above, and $n=1$, and $t=\tau=10$ min.).

The second approximation of the trajectory for the first 10 minutes was made by using averages of $u_{g0}+u_1$ and $v_{g0}+v_1$. Values of u_{g1} and v_{g1} were then obtained at the end of the second approximate trajectory to see if they were about the same as those at the end of the first approximate trajectory. If not, the new values of u_{g1} and v_{g1}, together with the original values of u_{g0} and v_{g0} and the mean latitude of the second approximate trajectory, were used in equations (5) and (6) to obtain new values of u_1 and v_1. The latter were averaged with u_{g0} and v_{g0}, respectively, to obtain the third approximation of the trajectory for the first 10 minutes. Values of u_{g1} and v_{g1} were measured at the end of this trajectory and compared with the values obtained for the second approximate trajectory. This procedure was continued until there was little or no change in the values of u_{g1} and v_{g1} in two successive approximations. The final approximation of the trajectory was then accepted as the true trajectory for the first 10 minutes.

The final computed values of u_1 and v_1 were used to construct the first approximation of the second 10-minute step of the trajectory. The procedure already described for the first 10-minute step was then followed, except that equations (5) and (6) were used without modification. Of course, for the second step of the trajectory, $n=2$ and $t=2\tau=20$ min. Succeeding steps of the trajectory were constructed in the same manner as the second step.

It may be easier to see qualitatively the effect on an air parcel moving relatively slowly when it enters a region of steep geopotential gradient by referring to figure 23. Assume a parcel of unit mass has moved horizontally from region A, where the geopotential gradient is weak, to point B, where the gradient is very strong, and has arrived at B with velocity **V**. The horizontal forces acting on the parcel at B, neglecting friction, will be the small Coriolis force $\mathbf{F}_c$ corresponding to **V**, acting at right angles to **V**, and the very large geopotential gradient force $\mathbf{F}_g$ acting at right angles to the contours. The net horizontal force on the parcel will be **F**, the vector sum of $\mathbf{F}_c$ and $\mathbf{F}_g$. Using natural coordinates with the positive normal axis directed to the left of the positive tangential axis, **F** may be resolved into a negative tangential force $\mathbf{F}_t$, tending to slow down the parcel, and a negative normal force $\mathbf{F}_n$, tending to make it move anticyclonically.

If $V=50$ kt.$=25.7$ m sec^{-1} and $\varphi=30°$, then $F_c=-2V\ \Omega \sin\varphi=-187\times10^{-5}$ m sec^{-2}, and $F_g=-\frac{\partial\Phi}{\partial n}=2V_g\ \Omega \sin\varphi$, where the forces are per unit mass. Taking an extreme case, let V_g at point B equal 1000 kt. or 515 m sec^{-1}. Then $F_g=3754\times10^{-5}$ m sec.$^{-2}$. By graphical solution, $|F|=|\mathbf{F}_c+\mathbf{F}_g|=3850\times10^{-5}$ m sec^{-2}, $F_t=-3350\times10^{-5}$ m sec^{-2}, and $F_n=-1880\times10^{-5}$ m sec^{-2}. Then, since for unit mass, $F_t=a_t=\frac{dV}{dt}$, $\Delta V=F_t\Delta t$, approximately. If $\Delta t=10$ minutes and the mean tangential force per unit mass on the parcel during this time is $\frac{F_t}{2}$,

$$\Delta V=\frac{-3350\times10^{-5}\times600}{2}=-10.1 \text{ m sec}^{-1}.$$

This indicates that the parcel must have had a speed of $25.7+10.1=35.8$ m sec^{-1} 10 minutes before arriving at point B and had slowed down while moving toward higher values of geopotential during the last 5 minutes of its trajectory.

The radius of curvature of the path of the parcel at B would be

$$R=\frac{V^2}{F_n}=\frac{(25.7)^2}{1880\times10^{-5}}=35.1\times10^3 \text{ m}=35.1 \text{ km}.$$